ing member of each pair identified as the desired iodide and smaller, slower member identified as the silyl pyridone starting material. Demethylation gave a pyridone mixture (M)-**7**, which resolved into two components on preparative separation over regular silica gel. Liquid chromatography–mass spectrometry analysis of the less polar fraction showed only four peaks, which were the four desired iodopyridones (M)-**7**. The more polar impurity fraction was not analyzed but is evidently a mixture of four products resulting from failure of trimethylsilyl/iodine exchange followed by successful demethylation.

The purified mixture was then reacted with one propargyl halide [R^2 = $Si(Me_2)CH{=}CH_2$]. This mixture (M)-**8** was purified again by silica gel flash chromatography. The purified mixture (M)-**8** was divided into five portions, and each was reacted with the five isonitriles in Fig. 3 to give five mixtures of four compounds each [(M)-**5**, R^2 = H]. The mixtures were then demixed as above after addition of the mappicine standard. Each mixture showed only the expected four peaks (20 out of 20 products formed, no impurities) in the expected order. The average four-step overall yield with two intermediate purifications was 6% [see the supplemental material for a table of all yields and retention times (*29*)]. In the experiment, all 20 products could be isolated in pure form by preparative demixing, which illustrates the potential benefits of intermediate mixture purification when nonquantitative reactions are involved.

Techniques like fluorous quasiracemic synthesis, which focus on a single mixture, can be used to leverage traditional synthetic research (such as natural product synthesis) by providing more than one product at the end. When used in a parallel synthesis like that of mappicine, fluorous mixture methods allow the synthesis of multiple complex scaffolds made as mixtures. These scaffold mixtures are then leveraged in the parallel synthesis stage by providing multiple products per vessel or well in good yield and excellent purity after demixing. Although this work describes only four-compound mixtures, the internal yield standard has a fifth tag, so it is already certain that five-compound mixtures can be made. On the basis of the steep gradient used and the peak separations in the HPLC library experiments, we think that expansion to at least 8- and possibly 10-compound mixtures should be straightforward.

References and Notes

1. I. T. Horváth, J. Rábai, *Science* 266, 72 (1994).
2. D. P. Curran, S. Hadida, *J. Am. Chem. Soc.* **118**, 2531 (1996).
3. I. T. Horváth, *Acc. Chem. Res.* **31**, 641 (1998).
4. A. Studer *et al.*, *Science* **275**, 823 (1997).
5. D. P. Curran, Z. Y. Luo, *J. Am. Chem. Soc.* **121**, 9069 (1999).
6. T. R. Govindachari, K. R. Ravindranath, N. Viswanathan, *J. Chem. Soc. Perkin Trans.* **1974**, 1215 (1974).
7. For leading reference to other isolation and synthesis work, see work by D. L. Boger and J. Y. Hong [*J. Am. Chem. Soc.* **120**, 1218 (1998)].
8. F. Balkenhohl, C. von dem Büssche-Hunnefeld, A. Lansky, C. Zechel, *Angew. Chem. Int. Ed. Engl.* **35**, 2289 (1996).
9. K. S. Lam, M. Lebl, V. Krchnak, *Chem. Rev.* **97**, 411 (1997).
10. A. Furka, in *Combinatorial Peptide and Nonpeptide Libraries*, G. Jung, Ed. (VCH, Weinheim, Germany, 1996), pp. 111–137.
11. K. C. Nicolaou, X. Y. Xiao, Z. Parandoosh, A. Senyei, M. P. Nova, *Angew. Chem. Int. Ed. Engl.* **34**, 2289 (1995).
12. D. P. Curran, *Angew. Chem. Int. Ed. Engl.* **37**, 1175 (1998).
13. D. Flynn, *Med. Res. Rev.* **19**, 408 (1999).
14. R. J. Booth, J. C. Hodges, *Acc. Chem. Res.* **32**, 18 (1999).
15. S. W. Kaldor, M. G. Siegel, *Curr. Opin. Chem. Biol.* **1**, 101 (1997).
16. Solution mixture techniques are used to make large discovery libraries, but these techniques cannot accommodate the isolation of individual pure compounds from the mixtures. Instead, libraries and sublibraries are made and tested in a process of deconvolution to identify interesting mixture components. For reviews, see (*17, 18*); for examples, see (*19, 20*).
17. R. A. Houghten *et al.*, *J. Med. Chem.* **42**, 3743 (1999).
18. H. An, P. D. Cook, *Chem. Rev.* **100**, 3311 (2000).
19. T. Carell, E. A. Wintner, A. Bashirhashemi, J. Rebek, *Angew. Chem. Int. Ed. Engl.* **33**, 2059 (1994).
20. D. L. Boger, W. Y. Chai, Q. Jin, *J. Am. Chem. Soc.* **120**, 7220 (1998).
21. Mixtures of organic compounds can of course be fractionated by chromatographic or other separation methods, but it is difficult or impossible to predict whether or how a mixture will separate. For fractionation of mixtures, see work by R. H. Griffith *et al.* [*Tetrahedron* **54**, 4067 (1998)].
22. The term "quasiracemic" follows from the definition of "quasiracemate" by Eliel and Wilen [see (*23*), p. 1205]. Quasienantiomers are used in parallel kinetic resolution [see (*24*)].
23. E. L. Eliel, S. H. Wilen, *Stereochemistry of Organic Compounds* (Wiley, New York, (1994).
24. E. Vedejs, X. Chen, *J. Am. Chem. Soc.* **119**, 2284 (1997).
25. H. Josien, S. B. Ko, D. Bom, D. P. Curran, *Chem. Eur. J.* **4**, 67 (1998).
26. H. Josien, D. P. Curran, *Tetrahedron* **53**, 8881 (1997).
27. O. de Frutos, D. P. Curran, *J. Comb. Chem.* **2**, 639 (2000).
28. D. P. Curran, M. Frauenkron, J.-H. Choi, A. Gabarda, unpublished results.
29. Supplemental material is available at www.sciencemag.org/cgi/content/full/291/5509/1766/DC1.

30. We thank the NIH for funding this work. Additional support through donations to the Center of Combinatorial Chemistry by Merck, Parke-Davis, and Hewlett-Packard is also appreciated. We also thank O. de Frutos for important preliminary experiments.

17 November 2000; accepted 26 January 2001

Reversible Surface Morphology Changes of a Photochromic Diarylethene Single Crystal by Photoirradiation

Masahiro Irie,* Seiya Kobatake, Masashi Horichi

The surface morphology of a diarylethene single crystal [1,2-bis(2,4-dimethyl-5-phenyl-3-thienyl)perfluorocyclopentene] determined by atomic force microscopy changed reversibly upon photoirradiation. The crystal underwent a thermally irreversible but photochemically reversible color change (colorless to blue) upon alternate irradiation with ultraviolet (wavelength λ = 366 nm) and visible (λ > 500 nm) light that drove reversible photocyclization reactions. Upon irradiation with 366-nm light, new steps appeared on the (100) single-crystalline surface that disappeared upon irradiation with visible light (λ > 500 nm). The step height, about 1 nm, corresponds to one molecular layer. Irradiation with 366-nm light formed valleys on the (010) surface that also disappeared by bleaching upon irradiation with visible light (λ > 500 nm). The surface morphological changes can be explained by the molecular structural changes of diarylethenes regularly packed in the single crystal. These crystals could potentially be used as photodriven nanometer-scale actuators.

Photochromism is the reversible transformation by photoirradiation of a chemical species between two forms that have different absorption spectra (*1, 2*). Among various photochromic materials, photochromic single crystals are of particular interest because of their potential usefulness for holographic and three-dimensional memories (*3–6*). Although various kinds of photochromic crystals have been developed (*3, 7–9*), crystals that undergo thermally irreversible photochromic reactions (*10*) are very rare. Recently, we have developed thermally irreversible and fatigue-resistant photochromic diarylethene crystals (*11–21*). The photoinduced coloration-decoloration cycles of the crystals can be repeated more than 10^4 times while maintaining the shape of the single crystals, and the photogenerated colored states are stable even at 100°C. During our studies of the single-crystalline photochromism, we found

Scheme 1.

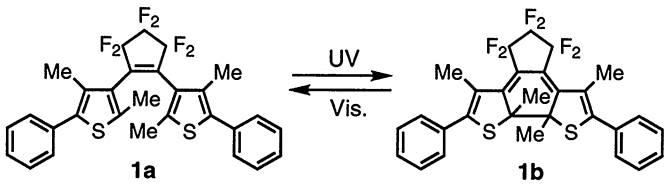

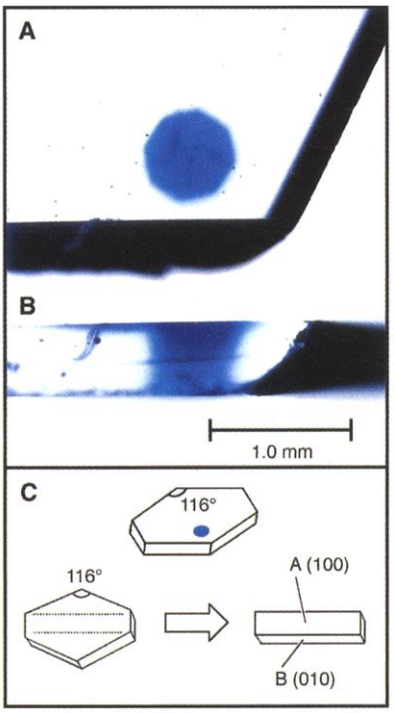

Fig. 1. Photographs of photoirradiated crystal **1**. (**A**) Top and (**B**) side views of the crystal; 366-nm light was used as the light source. (**C**) The shape of the crystal.

that some of the diarylethene single crystals showed reversible surface morphological changes when alternately irradiated with ultraviolet (UV) and visible light. Here, we report on the atomic force microscopy (AFM) study of the morphological changes and the molecular mechanism as assessed by x-ray crystallographic analysis. The reversible morphological changes are potentially applicable to photodriven, nanometer-scale actuators.

Morphological changes of photoreactive single-crystal surfaces were reported initially by Kaupp (*22*), who found that photodimerizations of *trans*-cinnamic acids (*23*) and anthracenes (*24, 25*) in the crystalline phase induced the surface morphological changes. The morphological changes were attributed to phase-rebuilding of the surface molecules upon photoisomerization. The changes were irreversible, however, and a critical claim that local heating may contribute to some extent to the morphological changes still remained (*26*). When the effect is reversible, the claim can be excluded.

The colorless single crystal of 1,2-bis(2,4-dimethyl-5-phenyl-3-thienyl)perfluorocyclopentene (**1a**) turned blue without change of the crystal shape upon irradiation with 366-nm light. The color change resulted from the formation of the closed-ring isomer (**1b**) (*27*). To confirm that the photoreaction (Scheme 1) takes place inside the crystal bulk, we observed the color change of a partially photoirradiated single crystal from both sides of the crystal (top view, Fig. 1A; side view, Fig. 1B). Upon irradiation with 366-nm light, the surface turned blue (Fig. 1A). The photographs clearly indicate that light penetrates the crystal into the bulk and induces the photoreaction as deep as 500 μm.

The shape of the crystal is shown in Fig. 1C. To determine the morphological changes that accompany the change in coloration, we measured surface A and sectional surface B with an atomic force microscope (*28*). The B surface was obtained by the cleavage of the crystal with a razor blade. The A surface of crystal **1a** before photoirradiation was flat (Fig. 2A). Upon irradiation for more than 10 s with 366-nm light (intensity 12 mW/cm^2), steps appeared on the surface (Figs. 2B and 3). Any step formation was not discerned during the initial 10-s irradiation but appeared after the induction period. The step height was 1.0 ± 0.1 nm. The step disappeared by bleaching upon irradiation with visible light ($\lambda > 500$ nm) (Fig. 2C). When the irradiation time was prolonged, the number of the steps increased and steps with heights of 2.0 ± 0.2 nm and 3.0 ± 0.3 nm appeared (Fig. 3). The height was always a multiple of the minimum step height (1.0 ± 0.1 nm), and we did not observe any steps with a height lower than the unit height (1.0 ± 0.1 nm). The morphological change was reversible and correlated with the color change of the crystal.

Department of Chemistry and Biochemistry, Graduate School of Engineering, Kyushu University, and CREST, Japan Science and Technology Corporation, Hakozaki 6-10-1, Higashi-ku, Fukuoka 812-8581, Japan.

*To whom correspondence should be addressed. E-mail: irie@cstf.kyushu-u.ac.jp

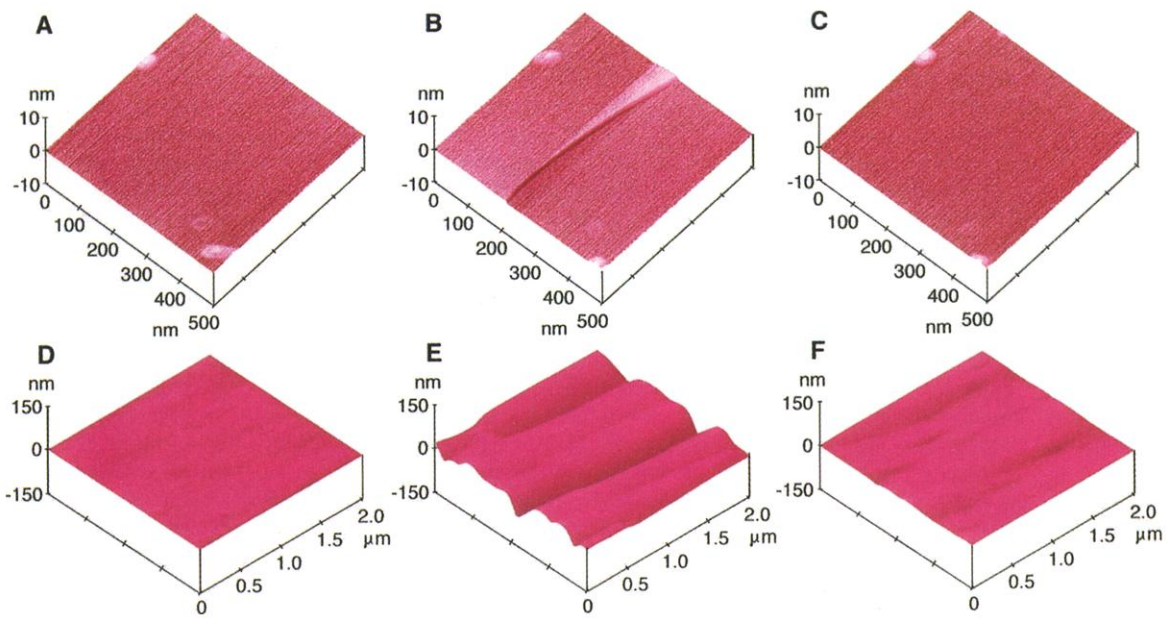

Fig. 2. AFM images of (**A** to **C**) the (100) crystal surface and (**D** to **F**) the (010) surface: before photoirradiation, (A) and (D); after irradiation with 366-nm light for (B) 10 s and (E) 15 s; and after irradiation with visible light ($\lambda > 500$ nm), (C) and (F).

The AFM images of the B surface before and after UV irradiation are shown in Fig. 2, D to F. Upon irradiation for 15 s with 366-nm light (intensity 12 mW/cm^2), the crystal turned blue and valleys appeared on the crystal surface. The depth of the valley was estimated to be 10 to 50 nm. The valley almost disappeared by bleaching upon irradiation with visible light ($\lambda > 500$ nm) (Fig. 2F). The morphological change was again reversible and correlated with the color change.

To determine the relation between the reversible formation of steps and valleys and photoisomerization of the diarylethene molecules, we carried out x-ray crystallographic analysis of **1a** and **1b** (*29*). Figure 4 shows the Oak Ridge Thermal Ellipsoid Plot (ORTEP) drawings of **1a** and **1b**. The distance between the reactive carbon atoms of **1a** was determined to be 0.396 nm, which is close enough for a photoreaction to occur (*30*). The face index of the A surface was determined to be (100). The sectional B surface corresponds to (010).

The molecular packing of the colorless open-ring isomers viewed from the A and B faces is shown in Fig. 5. Because of the difficulty of determining in situ the structure of the photogenerated closed-ring isomer in the open-ring isomer **1a** crystal by x-ray crystallographic analysis, we carried out absorption anisotropy (polar plot) measurement (*14, 15*) of the UV-irradiated single crystal to determine the structural change. The blue arrows in Fig. 5, A and B, show the direction of the transition moment vectors at 630 nm of the closed-ring isomers derived from the polar plots viewed from the A and B faces. The direction of the arrows coincided with the direction of the long axis of the colorless open-ring isomers, so that each molecule can undergo the cyclization reaction while remaining in the same position.

In previous studies (*14, 18*) we reported

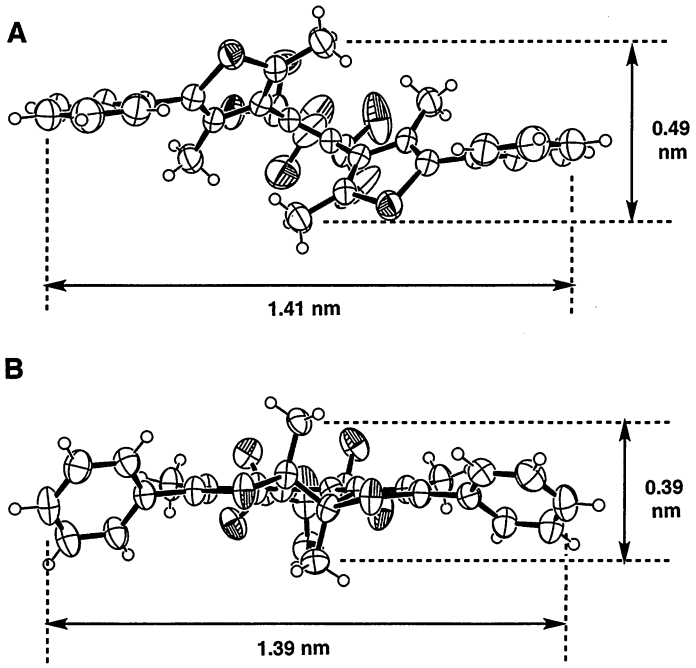

Fig. 4. ORTEP drawings of (**A**) **1a** and (**B**) **1b** showing 50% probability displacement ellipsoids.

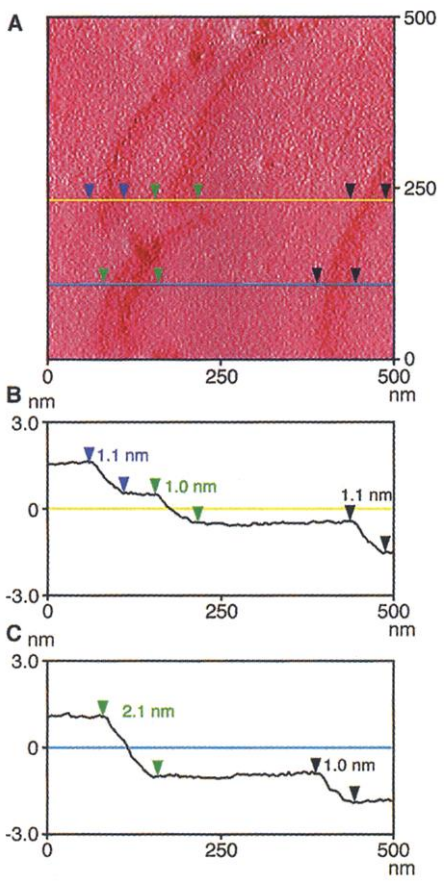

Fig. 3. AFM images of multisteps formed on the (100) crystal surface by irradiation with 366-nm light for 60 s. (**A**) Top view; (**B** and **C**) sectional views. These steps disappeared and the surface became flat after irradiation with visible light ($\lambda > 500$ nm).

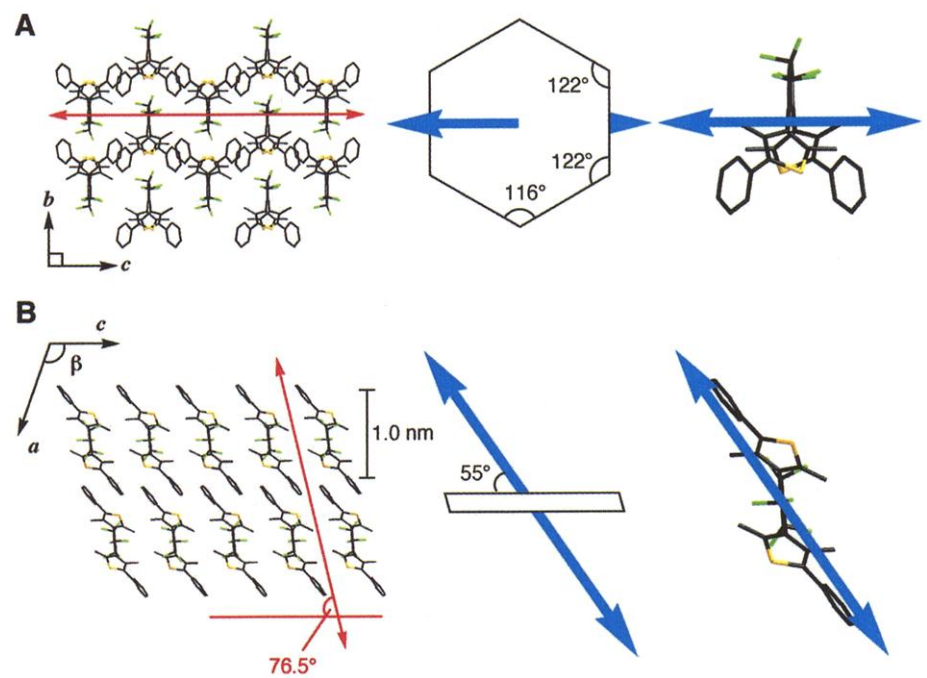

Fig. 5. Packing diagram of the (100) surface (**A**) and (010) surface (**B**) of **1a**, which correspond to A and B surfaces, respectively. Red arrows show the directions of formation of steps or valleys; blue arrows show the direction of the transition moment of 630-nm absorption. Typical molecular structures of packed **1a** are also shown at the right. Sulfur and fluorine atoms are shown by yellow- and green sticks, respectively. Hydrogen atoms are omitted for clarity.

that the distance between the 5- and 5′-carbons of the two thiophene rings of 1,2-bis(2,5-dimethyl-3-thienyl)perfluorocyclopentene is shortened as much as ~10%, and unit cell lengths and volume tend to decrease during the cyclization reaction in the crystal. X-ray crystallographic analysis of **1b** similarly confirmed that the distance between the edges of two phenyl rings was shortened from 1.41 to 1.39 nm when **1a** was converted to **1b** (Fig. 4). The cofacial orientation of the coplanar planes of **1b** (Fig. 5B) allows the molecules to pack each other closely, which decreases the unit cell along the *c* axis. This effect would explain the valley formation on the sectional B surface after UV irradiation. The direction of the valley is the same as the direction of the red arrow in Fig. 5B (76.5° tilted from the *b*-*c* plane) to within ±2°. Upon visible-light irradiation, the thiophene rings again rotated to the twisted conformation and expanded the *c* axis to fill up the valley.

The shortening in the distance between the phenyl ring edges by the cyclization reaction results in the decrease in the thickness of the molecular layers shown in Fig. 5B. The shrinking of the molecular layers produces vacancies in the crystal bulk. Accumulation of vacancies deep within the crystal allows the surface molecular layer to sink as much as one layer (~1 nm). According to the geometrical structural change shown in Fig. 4, the one-layer vacancy requires the photocyclization reactions of at least 60 molecular layers. Irradiation for 10 s with 366-nm light (intensity 12 mW/cm^2) induces the photocyclization reactions of 1.0×10^{17} molecules/cm^2 in the single crystal by taking into account 50% transmittance of the thin crystal at 366-nm light and the quantum yield of 0.96 (*21*). This corresponds to the photocyclization reactions of 600 molecular layers. The reactions take place as deep as 500 μm (Fig. 1). Therefore, the reacted molecules are not localized in the 600 layers but are distributed in about 5×10^5 layers (= 500 μm). The number of reacted molecules in 600 (versus 60) molecular layers is necessary to produce the one–molecular layer vacancy. When the number of reacted molecules is less than 1.0×10^{17} molecules/cm^2, the steps have been barely formed. The induction period is the accumulation time of the reacted molecules until 1.0×10^{17} molecules/cm^2. This process would explain step formation on the A crystal surface. Upon prolonged irradiation, the vacancies increase and two or more molecular layers sink. The direction of the step formation was along the *c* axis (Fig. 5A, red arrow). The rather weak interaction between perfluorocyclopentene groups possibly induces the step formation along the *c* axis. The cycloreversion reaction filled up the vacancies, and the surface with steps again returned to the initial flat surface.

The crystal reversibly shrank and expanded by alternate irradiation with UV and visible light. The shrinkage of the surface was digital, and each step corresponded to the thickness of one molecular layer as short as 1 nm. The reversible surface morphological changes could be applied to photodriven, nanoscale actuators that reversibly change thickness stepwise by alternate irradiation with UV and visible light.

References and Notes

1. G. H. Brown, *Photochromism* (Wiley-Interscience, New York, 1971).
2. H. Dürr, H. Bouas-Laurent, *Photochromism. Molecules and Systems* (Elsevier, Amsterdam, 1990).
3. W. J. Tomlinson, E. A. Chandross, R. L. Fork, C. A. Pryde, A. A. Lamola, *Appl. Opt.* **11**, 533 (1972).
4. M. Irie, *Photo-Reactive Materials for Ultrahigh-Density Optical Memory* (Elsevier, Amsterdam, 1994).
5. D. Psaltis, F. Mok, *Sci. Am.* **273**, 52 (November 1995).
6. S. Kawata, Y. Kawata, *Chem. Rev.* **100**, 1777 (2000).
7. T. Kawato, H. Koyama, H. Kanatomi, M. Isshiki, *J. Photochem.* **28**, 103 (1985).
8. J. R. Scheffer, P. R. Pokkuluri, in *Photochemistry in Organized & Constrained Media*, V. Ramamurthy, Ed. (VCH, New York, 1990), pp. 185–246.
9. J. Harada, H. Uekusa, Y. Ohashi, *J. Am. Chem. Soc.* **121**, 5809 (1999).
10. "Thermally irreversible photochromic reactions" mean that both isomer forms resist thermal reactions but photochemically interconvert each other.
11. M. Irie, *Chem. Rev.* **100**, 1685 (2000).
12. _____, K. Uchida, T. Eriguchi, H. Tsuzuki, *Chem. Lett.* (no. 10), 899 (1995).
13. M. Irie, K. Uchida, *Bull. Chem. Soc. Jpn.* **71**, 985 (1998).
14. S. Kobatake, T. Yamada, K. Uchida, N. Kato, M. Irie, *J. Am. Chem. Soc.* **121**, 2380 (1999).
15. S. Kobatake, M. Yamada, T. Yamada, M. Irie, *J. Am. Chem. Soc.* **121**, 8450 (1999).
16. T. Yamada, S. Kobatake, K. Muto, M. Irie, *J. Am. Chem. Soc.* **122**, 1589 (2000).
17. M. Irie, T. Lifka, S. Kobatake, N. Kato, *J. Am. Chem. Soc.* **122**, 4871 (2000).
18. T. Yamada, S. Kobatake, M. Irie, *Bull. Chem. Soc. Jpn.* **73**, 2179 (2000).
19. T. Kodani, K. Matsuda, T. Yamada, S. Kobatake, M. Irie, *J. Am. Chem. Soc.* **122**, 9631 (2000).
20. S. Kobatake, K. Shibata, K. Uchida, M. Irie, *J. Am. Chem. Soc.* **122**, 12135 (2000).
21. K. Shibata, K. Muto, S. Kobatake, M. Irie, in preparation.
22. G. Kaupp, in *Advances in Photochemistry*, D. C. Neckers, D. H. Volman, G. von Bünan, Eds. (Wiley-Interscience, New York, 1994), vol. 19, pp. 119–177.
23. _____, *Angew. Chem. Int. Ed. Engl.* **31**, 592 (1992).
24. _____, *Angew. Chem. Int. Ed. Engl.* **31**, 595 (1992).
25. _____, M. Plagmann, *J. Photochem. Photobiol. A* **80**, 399 (1994).
26. L. Jiang *et al.*, *Adv. Mater.* **11**, 649 (1999).
27. M. Irie, K. Sakemura, M. Okinaka, K. Uchida, *J. Org. Chem.* **60**, 8305 (1995).
28. The morphological change of a crystal surface by AFM was measured with a Digital Instruments NanoScope IIIa scanning probe microscope in tapping mode. Commercial standard etched silicon tips (cantilever length = 125 μm, resonance frequency ~ 350 kHz) were used as a cantilever of AFM. Photoirradiation was carried out using a fiber mercury-Xe lamp (200 W) as the light source; the irradiation wavelength was selected with bandpass filters.
29. X-ray crystallographic analysis was carried out using a Bruker SMART1000 charge-coupled device–based diffractometer (50 kV, 40 mA) with Mo Kα radiation. Crystal data for **1a**: $C_{29}H_{22}F_6S_2$, MW = 548.59, monoclinic, space group *C2/c*, $Z = 4$, $T = 298(2)$ K, $a = 24.023(4)$ Å, $b = 8.466(2)$ Å, $c = 13.350(2)$ Å, $\beta = 109.235(3)°$, $V = 2563.6(8)$ Å^3, goodness of fit = 0.944, $R1[I > 2\sigma(I)] = 0.0485$, *wR2* (all data) = 0.1421. Crystal data for **1b**: $C_{29}H_{22}F_6S_2$, MW = 548.59, monoclinic, space group $P2_1/c$, $Z = 4$, $T = 296(2)$ K, $a = 18.472(6)$ Å, $b = 10.884(2)$ Å, $c = 10.659(3)$ Å, $\beta = 100.87(3)°$, $V = 2491.3(11)$ Å^3, goodness of fit = 1.051, $R1[I > 2\sigma(I)] = 0.0794$, *wR2* (all data) = 0.2259. Crystallographic data (excluding structure factors) for the structures in this paper have been deposited with the Cambridge Crystallographic Data Centre as supplementary publications CCDC 155979 and 155980. Copies of the data can be obtained, free of charge, from CCDC (e-mail: deposit@ccdc.cam.ac.uk). Details of x-ray crystallographic analysis are also available at *Science* online (www.sciencemag.org/cgi/content/full/291/5509/1769/DC1).
30. V. Ramamurthy, K. Venkatesan, *Chem. Rev.* **87**, 433 (1987).

31. Supported by CREST (Core Research for Evolutional Science and Technology) of Japan Science and Technology Corporation (JST) and by Grant-in-Aid for Scientific Research 12131211 from the Ministry of Education, Culture, Sports, Science and Technology, Japan.

21 November 2000; accepted 22 January 2001

Ablation, Flux, and Atmospheric Implications of Meteors Inferred from Stratospheric Aerosol

D. J. Cziczo,[1,2] D. S. Thomson,[1,2] D. M. Murphy[1]*

Single-particle analyses of stratospheric aerosol show that about half of the particles contain 0.5 to 1.0 weight percent meteoritic iron by mass, requiring a total extraterrestrial influx of 8 to 38 gigagrams per year. The sodium/iron ratio in these stratospheric particles is higher and the magnesium/iron and calcium/iron ratios are lower than in chondritic meteorites, implying that the fraction of material that is ablated must lie at the low end of previous estimates and that the extraterrestrial component that resides in the mesosphere and stratosphere is not of chondritic composition.

Accurate measurement of the flux of interplanetary material to Earth has proven difficult because the majority of extraterrestrial matter incident on the atmosphere is in the form of micrometeors that ablate at ~100-km altitude when atmospheric pressure causes sufficient frictional heating (*1*–*6*). Only a minor fraction reach the surface without va-